Received Date : 03-May-2016
Accepted Date : 07-Nov-2016
Article type : Primary Research Articles

Going with the flow: The role of ocean circulation in global marine ecosystems under a changing climate

Running head: Changing ocean circulation and ecosystems

Authors

S.J. van Gennip[1], E.E. Popova[1], A. Yool[1], G.T. Pecl[2], A.J. Hobday[3], C.J.B. Sorte[4]

[1] National Oceanography Centre, University of Southampton Waterfront Campus, European Way, Southampton, SO14 3ZH, UK

[2] Institute for Marine and Antarctic Studies, University of Tasmania, PO Box 49, Hobart, Tasmania, 7001, Australia

[3] CSIRO Oceans and Atmosphere, Hobart, Tasmania, 7000, Australia

[4] University of California, Irvine, 321 Steinhaus Hall, Irvine, CA 92697-2525, USA

Corresponding author:

Simon van Gennip; tel: +44 (0) 2380 596 611, email: s.van.gennip@noc.ac.uk

Keywords: climate change, global ocean circulation model, larval dispersal range, coastal connectivity, ecosystems

Abstract

Ocean warming, acidification, deoxygenation and reduced productivity are widely considered to be the major stressors to ocean ecosystems induced by emissions of CO_2. However, an overlooked stressor is the change in ocean circulation in response to climate change. Strong changes in the intensity and position of the western boundary currents have already been observed, and the consequences of such changes for ecosystems are beginning to emerge. In this study, we address climatically induced changes in ocean circulation on a global scale but relevant to propagule dispersal for species inhabiting global shelf ecosystems, using a high resolution global ocean model run under the IPCC RCP 8.5 scenario. The ¼ degree model resolution allows improved regional realism of the ocean circulation beyond that of available CMIP5-class models. We use a Lagrangian approach forced by modelled ocean circulation to simulate the circulation pathways that disperse planktonic life stages. Based on trajectory backtracking, we identify present-day coastal retention, dominant flow and dispersal range for coastal regions at the global scale. Projecting into the future, we identify areas of the strongest projected circulation change and present regional examples with the most significant modifications in their dominant pathways. Climatically-induced changes in ocean circulation should be considered as an additional stressor of marine ecosystems in a similar way to ocean warming or acidification.

Introduction

Impacts of climate change are currently manifesting across all major marine ecosystems around the world (e.g. Wassmann, 2011; IPCC, 2013; Hoegh-Guldberg & Bruno, 2014; Okey, 2014; Pecl *et al.*, 2014). A growing body of evidence demonstrates that human-caused changes, primarily rising temperatures, are already leading to profound and potentially irreversible modifications to marine ecosystems, with consequences both for biodiversity and the dependent human systems. Ocean warming, acidification, deoxygenation and reduced productivity (resulting from increased stratification) are widely considered to be the key stressors as a result of anthropogenic emissions of CO_2 (e.g. Bopp *et al.*, 2013). However, climatically-driven change to ocean circulation is an important additional stressor, and potentially the primary one in certain locations (Popova *et al.*, 2016). Strong changes in intensity and in position of western boundary currents have already been observed (Wu *et al.*, 2012), and their consequences for ecosystems are beginning to emerge (e.g. Banks *et al.*, 2010, Matear *et al.*, 2013; Popova *et al.*, 2016).

One western boundary current, the East Australian Current (EAC), provides one of the most pronounced examples of such a stressor. The poleward flowing EAC-extension has increased in strength since the 1940's (Ridgway, 2007; Hill *et al.*, 2008) despite little change in the overall volume of the core EAC region (Sloyan and O'Kane, 2015). Major changes in regional ecosystem dynamics have been attributed to these changes in advection and associated regional warming (e.g. Thompson *et al.*, 2009; Ling *et al.*, 2009; Johnson *et al.*, 2011; Marzloff *et al.*, 2016). While changes to circulation can act to accelerate climatically-driven temperature rises, the impacts observed around the EAC are above and beyond those attributable to this warming alone. Furthermore, climate models project changes to continue in the EAC (e.g. Popova *et al.*, 2016), including an increase in strength of 12% in the core area and 35% in the EAC poleward extension by 2060 (Sun *et al.*, 2012).

Changes in ocean circulation affect marine ecosystems through the dispersal of reproductive or juvenile life stages. The majority of marine species have complex life cycles involving a pelagic larval stage that persists for up to a year (Pechenik, 1999; Kinlan & Gaines, 2003; Cowen *et al.*, 2007), and in some cases longer (e.g. the spiny lobsters that underpin many valuable fisheries have larval durations of one year and greater, Rudorff *et al.*, 2009; Bradford *et al.*, 2015). In the earliest life stages, these larvae are often largely passive – or near-passive – drifters that are dispersed by ocean currents (Marshall & Morgan, 2011). Such larval dispersal may be critical for population persistence as it enables exchange of individuals – that is, connectivity – across a broader metapopulation (Lett *et al.*, 2010; Goldwyn and Hastings 2011). Marine populations in particular areas are thus not necessarily locally self-sustaining but instead are often dependent on the transport of new individuals via ocean currents.

Observations of the larvae of shallow-water species in ocean gyre systems suggests that dispersal is possible on scales stretching to hundreds and even a thousand kilometres (Cowen, 2007; Kinlan & Gaines, 2003, and references therein). Dynamics and variability of western and eastern boundary currents, circumpolar and large-scale gyre circulation mediate population connectivity at the basin scale (e.g. Werner *et al.*, 2007, and references therein). Thus, change of large-scale circulation under a warming climate is likely to directly influence marine population dynamics, including the “propagule pressure” of invasive species to a given area, or of native species extending distributions into new areas as the climate changes (Bates *et al.*, 2014).

Projecting the future impact of changes in ocean circulation for coastal marine systems is challenging, and few modelling studies to date have considered this as an additional stressor of ocean ecosystems (e.g. Gerber *et al.*, 2014; Cetina-Heredia *et al.*, 2015; Popova *et al.*, 2016). While diagnosing a change in the strength and position of major currents in future projections of ocean models is a reasonably straightforward task, relating such change to impacts on ocean ecosystems is more difficult. Running complex models of biological behaviour in parallel with that of global climate models at a resolution sufficient to meaningfully resolve current systems, requires significant computational resources (e.g. Munday *et al.*, 2009; Gerber *et al.*, 2014). However, viewing circulation change from a Lagrangian frame-of-reference is a practical approach to investigate how global circulation change may influence ecosystem dynamics (e.g. Kendall *et al.*, 2015).

Ecosystem dynamics and functioning are put under pressure as climate-driven ocean warming modifies the thermal landscape, forcing species to migrate to follow their thermal niche. Sorte (2013) highlights the importance of the flow directionality – through propagule dispersal – in facilitating the extension of species range boundaries depending on whether the flow follows or is opposite to the direction of climate change (i.e. predominantly poleward). As climate change warms ocean waters, coastal species living along poleward flowing currents may benefit from the opportunity this affords to reach cooler waters. However, it remains unclear how climate-driven ocean circulation changes may modify such pathways.

In this study, we aim to address how climatically-induced changes in ocean circulation may affect propagule dispersal for species inhabiting shelf ecosystems focusing on the meridional direction using a Lagrangian approach. We take advantage of an eddy-permitting global ocean model forced by output from an Earth System Model (ESM) run under the strong warming RCP 8.5 scenario (Rogelj *et al.*, 2012). The model's horizontal resolution of ¼-

degree allows good regional realism of ocean circulation and an improvement in shelf dynamics over that possible in CMIP5-class models used in the most recent synthesis by the Intergovernmental Panel on Climate Change (IPCC) Assessment Report 5 (AR5).

Materials and methods

High resolution ocean projection

Our ocean projection uses the Nucleus for European Modelling of the Ocean (NEMO) framework. This is comprised of an ocean general circulation model (OGCM), OPA (Madec, 2008), coupled with a sea-ice model, LIM2 (Timmermann *et al.*, 2005). NEMO version 3.5 is used here with a horizontal resolution of approximately 1/4° and a vertical grid of 75 levels increasing from 1 m thickness at the surface to 200 m at abyssal depths. The model is run from 1975 until 2099 under the strong warming RCP8.5 scenario (Yool *et al.*, 2013, Yool *et al.*, 2015). Further details concerning model configuration, forcing and validation can be found in Appendix S1.

With specific reference to ocean circulation, Figure 1 presents decadal-averaged surface currents for both NEMO and the Aviso geostrophic velocity product (AVISO, 2014, Appendix S2). The velocities shown are on the same scale, and represent the period 2000-2009, though note that the comparison is illustrative of general patterns and magnitudes only since the model cannot (and does not attempt to) represent the precise period and variability for 2000-2009. The model shows good skill in reproducing major circulation features of ocean dynamics, such as boundary currents, and the Antarctic Circumpolar Current (ACC). Nonetheless, NEMO still poorly resolves a number of features and details of surface circulation. For example, details of circulation – such as the Gulf Stream separation at Cape

Hatteras – are slightly misplaced spatially. More generally, the model underestimates spatial variability, both of fast surface currents and in the relatively quiescent gyre areas. For the latter, the model, though eddy-permitting, still cannot properly resolve eddy activity, a deficiency rooted in resolution that is underscored by higher-resolution instances of NEMO which resolve eddies directly (Marzocchi *et al.*, 2015). Nonetheless, the increased resolution used here permits a considerable improvement in the representation of ocean circulation over that of lower resolution climate models (cf. Yool *et al.*, 2015).

Lagrangian calculations

Ocean currents are highly variable in time and space with modes of variability that range from days to centuries. As such, it is difficult to infer advective pathways directly from the speed and direction of the ocean currents evolving in time. Even more challenging is to interpret how an intensification and/or a shift of a meandering current may impact the origin and fate of advected particles. In order to translate changes in Eulerian velocities (i.e., at a fixed point) – which are a standard output of ocean general circulation models – into advective pathways that are more relevant to the transport of marine organisms, we employ a Lagrangian approach (Siegel *et al.*, 2003). In this, the main ocean circulation pathways (and associated timescales) are obtained through analysing the trajectories of more than 8.1 million point particles that are “released” and “tracked” into the model’s 3-dimensionnal flow field.

To calculate these Lagrangian trajectories, we use an offline, mass-preserving scheme, ARIANE (http://stockage.univ-brest.fr/~grima/Ariane/). Detailed descriptions of the ARIANE algorithm are given in Döös (1995) and Blanke & Raynaud (1997). Lagrangian diagnoses are derived using five-day mean velocity fields of the high-resolution global model described previously. Such a Lagrangian analysis has been carried out successfully in a variety of global and regional ocean circulation studies relevant to a variety of biogeochemical problems (Johnson *et al.*, 2011, Popova *et al.*, 2013, Jutzeler *et al.*, 2014, Cetina-Heredia *et al.*, 2015, Srokosz *et al.*, 2015, Doblin & van Sebille, 2016, Robinson *et al.*, 2016).

We assessed the model Lagrangian transport (Appendix S3, Fig. S1) and show how key characteristics of trajectories compare to those obtained from drifters data from the NOAA Global Drifting Program (http://www.aoml.noaa.gov/phod/dac/) (Lumpkin *et al.*, 2012).

Experiment design

We focus our study on a relatively narrow strip (given the global scale) along coastal margins where the impact of changing circulation will be of utmost importance for living marine resources and communities dependent on them, and where current and future cumulative anthropogenic impacts are greatest. While the Lagrangian particles are released in this focused region, their trajectories are then tracked globally. The particles can be considered as representation of any passive (lacking own ability to move) component of the system whose motions are dominated by the flow. Here, particles represent planktonic life stages of organisms, but the technique, as well as the dataset produced here, can be used to consider other subjects such as nutrients (e.g. Robinson *et al.*, 2014).

Particles are deployed near-surface (at 2 m depth), along the entire global coastline and around major islands in a ribbon-like manner, 70 km off the coast at sites spaced 1 km apart (Fig. 2). The choice of particle release away from the coast reflects limitations in representing near-shore processes in global-scale NEMO – that is, a trade-off between representing coastal areas well but regionally versus less well but globally. We effectively assume that unmodelled near-shore processes will transport larvae to this distance from the coast, at which point model-resolved circulation is the dominant factor for dispersal. The choice of a fixed 70 km distance rather than the shelf edge was made in acknowledgement of the diversity in size of shelf regions. Rather than start particles at a range of distances from the coast (as would occur by using the shelf edge), we selected a fixed distance to avoid biasing our analysis. The Arctic and Antarctic are omitted from the analysis because circulation in these areas is largely zonal (i.e. east-west) rather than meridional (i.e. north-south; the focus of our study). The Mediterranean, Baltic, East China, Japan and Okhotsk seas are excluded because they are semi-enclosed with limited “ventilation” to the World Ocean.

Particles are deployed at four regular time intervals each year (1st Jan, 1st April, 1st July and 1st October) for a full decade in order to capture seasonal and interannual variability. To evaluate the influence of climate change, we examine two decades at either end of the 21st century: 2000-09 (used as a reference) and 2090-99. Lagrangian tracking is performed in backtracking mode, and thus, we study the origin and trajectory of the particles reaching the coastal site rather than leaving it. Once released, particles are backtracked for 12 months with their trajectories (horizontal location and depth) recorded at 5-day intervals.

For the analysis, we grouped the trajectories of release sites into 50 km long sections of coast. For example, we positioned 23,154 sites along the South American coast generating 454 sections. Each section of coast contains 50 sites, with each having trajectories from 40 releases (i.e. 10 years of 4 releases per year). For each section, this generates a total of 2,000 trajectories that permit a probabilistic analysis of circulation. An example of trajectories released from a single 50 km section is shown in Figure 2b-d**.** For our global analysis, 4,078 sections were examined (Fig. 2a), resulting in 203,900 release sites, and 8,156,000 trajectories.

We studied the trajectories of the particles for 3, 6 and 12 months. These time scales were selected to encompass a range of pelagic larval durations (e.g. Cowen *et al.*, 2007). We focus in this paper on the results from the 6 month trajectories. The resulting dataset – including the periods 2000-09, 2050-59 and 2090-99 with trajectories of particles for up to 12 months – is available in ASCII format from the Dryad Digital Repository (http://dx.doi.org/10.5061/dryad.233hb). This allows the development of alternative metrics of circulation impact on the marine life forms or more detailed studies of specific regions. In addition, the dataset may serve to facilitate further model intercomparison studies.

Why is a global approach needed?

Figure 2 illustrates the 6-month dispersal of particles from a globally-distributed subset of the sections examined. At this intermediate timescale, basin-scale propagation is widespread, and particle dispersal is strongly affected by features such as boundary / coastal currents and equatorial upwelling regions. This demonstrates that dispersal is not confined to the shelf, and that a global-scale model is best suited to produce a synoptic intercomparison of coastal areas. Several contemporary examinations of population connectivity in biological systems also note basin-scale connectivity and highlight links between populations at larger scales than anticipated (Coleman *et al.*, 2013; Botsford *et al.*, 1994; Saunders, 2014).

Metrics of circulation impact

We developed three metrics to describe the impact of climate change on circulation regimes at the global scale which are relevant to issues of connectivity (metric 1) and dispersal with focus on the latitudinal direction (metric 2 and 3). Details and rationale for these metrics are given in the following sections.

Metric 1: Coastal retention level

In our simulations, particle trajectories are calculated backwards in time, such that we know that all particles reach a particular location at a particular time, which allows us to determine the source of particles reaching a specific place. Our first metric examines all incoming 6-month trajectories for a given site and determines the proportion that originates from coastal waters. Coastal waters here are defined as within 85 km from shore, corresponding to the average width of the global coastal shelf (Walsh, 1991, Elrod *et al.*, 2004). Figure S2 shows the origin location of all particles 6 months before ending at a coastal site in Iceland. In total, 41 % of particles originated from coastal waters which includes the Icelandic but also the Greenland coast. Coastal retention was calculated for the entire global coast.

Metric 2: Dominant latitudinal direction

Our second metric identifies the latitudinal direction of the dominant flow and quantifies the “strength” of this flow, defined here as the ability of the current to preclude upstream trajectories. We define the dominant latitudinal direction of the flow at a particular location as the proportion of particles that have travelled poleward to end up at that particular location (See appendix S4 for details).

Values above 50% indicate poleward flow, whereas values below 50% show locations where equatorward flow is dominant. Those close to 50% are characteristic of "multidirectional flows", meaning that particles are equally likely to move poleward or equatorward. In the context of climate change, poleward flow moves in the same general direction as climate change, and may facilitate the relocation of species to match changing preferred thermal regimes.

Figure 3 shows an example of the dominant flow direction metrics calculated for the Chilean coast. Averaged across the 6-month period, 29% of particles have travelled poleward to reach the site, whilst the other 71% have travelled equatorward, showing a dominant latitudinal direction of the flow towards the equator.

Metric 3: Poleward/Equatorward circulation dispersal range

For this metric, we obtain two values: the maximum Poleward (MPD) and the maximum Equatorward (MED) dispersal range for each site. The objective is to quantify the maximum meridional distance that a propagule inhabiting coastal waters can potentially be advected by the flow to reach a given coastal location.

To calculate the MPD for a given site S with coordinates (X_s,Y_s), we first identify in each trajectory the position of each point relative to the coast to only consider those within 85 km from the shore. We then select among these points in each trajectory i the position $(\mathrm{Xe}_i, \mathrm{Ye}_i)$ with latitude closest to the equator and generate a distribution with values from all trajectories (Fig. 3). Finally, we use the mean latitude of the most extreme 1% ($\overline{\mathrm{Ye}}_{1\%}$) of this distribution to calculate the latitudinal displacement required to reach S, such that:

$$\mathrm{MPD} = \left|\overline{\mathrm{Ye}}_{1\%} - \mathrm{Y}_s\right| .$$

Similarly, we obtain MED:

$$\mathrm{MED} = \left|\overline{\mathrm{Yp}}_{1\%} - \mathrm{Y}_s\right| ,$$

where ($\overline{\mathrm{Yp}}_{1\%}$) corresponds to 1% of latitude values in the distribution that is generated using the point ($\mathrm{Xp}_i, \mathrm{Yp}_i$) in each trajectory located most towards the pole. MPD and MED are expressed in degrees of latitude. Note that for this metric, we only considered the trajectories' coastal points so to obtain realistic coastal species propagule displacement. In regions of low coastal retention levels (metric 1), many trajectories come from open waters and only have a few coastal points, those when the particle nearly reaches the site. The 1% threshold was chosen to identify the group of particles most likely to populate distant new suitable areas and therefore to extend the species range boundaries. Further analysis found this result insensitive to higher thresholds or to the use of single trajectory statistics such as the 99th percentile (see Fig. S3).

Figure 3 shows an illustration of latitudinal dispersal range with the minimum and maximum latitude of each trajectory plotted in blue and red respectively, and with the extreme 1% of each distribution highlighted. Maximum poleward and equatorward displacements are equal to 7.0° and 5.6° for this site, indicating that, although the dominant latitudinal direction is equatorward, outlier particles are dispersed in both poleward and equatorward directions.

Results

Period 2000-09

Metric 1: Coastal retention levels

Speed, flow direction relative to the coast and distance between neighbouring coastlines greatly influence the origin – coast or open water – of incoming particles. Coastal retention levels are very low (<10% of trajectories) in regions where the dominant current is perpendicular to the coast such as coastal regions to the east of equatorial currents. Regions on the East African coast directly exposed to the Indian Equatorial Current show retention levels < 10% due to the large influx of open waters. This is also true for regions further north (Somalian Coast) and south (east South Africa, West Madagascar) due to the fast speed of the boundary currents it generates. Similar patterns are observed in the western Atlantic and Pacific, with low levels along the Brazilian and Northeast Australian coast, respectively. Low retention levels are also present for islands located far from the continental coast (Iceland, new Zealand, Falkland).

In contrast coastal retention is high (> 70 % of particles) where currents are relatively slower and follow the coast. These are mainly along eastern boundary currents (Californian, Chilean and Angola coast) or at the confluence of two major currents (Argentinian shelf).

Metric 2: Dominant flow direction

In principle, dominant latitudinal direction of the flow can vary between 0 % (no particle flowing polewards) and 100 % (all particles moving polewards). However, due to its strong spatiotemporal variability, ocean flow over seasonal time scales is never completely one-directional. As can be seen from Figure 4b, there are substantial stretches of the global coastline (28% of the total domain considered) where flow has a pronounced dominant direction, either poleward or equatorward (here we define “pronounced” as <10% or >90%).

The most notable areas are found along major Western Boundary Currents: the Agulhas Current along the east coast of South Africa with ~3200 km of uninterrupted pronounced poleward flow; the North-Brazil Current from Venezuela to French Guiana (~3100 km); the Gulf Stream along the east coast of the United States of America from the tip of Florida to Cape Hatteras, North Carolina (~1700 km); the Kuroshio along the eastern coast of Japan (~1800 km). Long stretches of pronounced poleward flow are also found along western continental margins, either along the eastern flanks of subpolar gyres or major Eastern Boundary Currents. For instance, the Alaska Current along the west Canadian coast (~1200 km) and the poleward-flowing Davidson Current (Clarke, 2013) within the California Current system (~900 km) in the Pacific; the Benguela Current System (~1500 km) and the Norwegian Atlantic Current (~1300 km) in the Atlantic; and the Leeuwin Current off the west Australian coast (~1900 km) in the Indian Ocean.

Long coastal areas with pronounced equatorward flow also exist, where less than 10% of particles move poleward due to equatorward-flowing currents. The most notable of these is in the northern North Atlantic, where the eastern Canadian coast is exposed to the southward-flowing Labrador Current. Here, ~3200 km of coastline have a pronounced equatorward flow and, after a short stretch, this flow continues past the Gulf of Saint Lawrence for a further ~850 km. Similarly, the eastern coast of Greenland (67°N–78°N) has ~1500 km of equatorward flow. In total, approximately 19% of the coastline investigated is dominated by pronounced poleward displacement and 9% is dominated by pronounced equatorward flow, with the rest of the global shelves (72%) exposed to weaker dominant flows.

Metric 3: Poleward/Equatorward circulation dispersal range

The second metric reflects the distance moved of the furthest-travelling (in a meridional sense) particles during the 6 months prior to arriving to each site. Note that only coastal data points were selected for this metric. The distribution of this metric along the global shelves is shown in Figure 4c, and is expressed in units of degrees latitude. The values of this metric vary up to 30 degrees of latitude (~3300 km in latitudinal direction) over the period of 6 months.

The distribution in Figure 4c is rich in details, with a clear general pattern showing pronounced clustering of long-distance particles in the proximity of the main boundary currents. The largest poleward dispersal distances (25-30 degrees over six months) occur in the vicinity of four of the five main Western Boundary Currents (the Gulf Stream, Agulhas, Kuroshio and East Australian Currents), as well as in the East Arabian and Caribbean Currents. Dispersal in the vicinity of the fifth main boundary current, the Brazil Current, does not show elevated values. This can be explained by the Brazil Current being a weak and narrow western boundary current dominated by eddies and by the seasonal variability associated with the position of the Southern Equatorial bifurcation - where the Brazil Current and northward-flowing North Brazil Current form (Rodrigues, 2007; Soutelino *et al.*, 2011). These features induce a complex, multi-directional propagation of the Lagrangian particles rather than a coherent single-directional flow as occurs in the vicinity of the main boundary currents. In addition, lower values can also be explained by the relatively closer position of the current to the equator resulting in particles partly travelling zonally in the South Equatorial Currrent current over timescales of 6 months.

Unsurprisingly, the smallest poleward dispersals occur in the vicinity of strong equatorward currents such as the Falklands, East Greenland, Labrador, Portugal and Canary Currents in the North Atlantic. Poleward dispersal is clearly most limited by the dominant current direction; however, even within these regions, only a small proportion of coast presents no poleward displacement potential (<1° covered in 6 months). The largest of these 'no-poleward-dispersal' zones is approximately 1500 km of coastline north of Newfoundland on the east Canadian coast.

The maximum range in the equatorward direction is shown in Figure 4d. Maximum equatorward displacement is slightly lower than maximum poleward displacement (Fig. 4c), and the extremes do not exceed 26 degrees over the period of six months. Similar to the maximum displacement in the poleward direction, the values also cluster along the main boundary currents. However, maximum displacements in equatorward and poleward directions are not simple mirror images of each other. Although the smallest values do occur along the main western boundary currents (with the Brazil Current again an exception here), it is noteworthy that equatorward-flowing eastern boundary currents (e.g. the Humboldt, Benguela, and California Currents) result in a relatively weak equatorward dispersal of only about 2-8 degrees over six months. This is a consequence of these currents being broader and more slowly flowing than western boundary currents. The largest values of equatorward dispersal occur in the vicinity of the equatorward-flowing East Greenland and Labrador currents (23-25 degrees).

Future changes in ocean circulation

Figure 1c shows the difference between the decadal-average surface current speed of 2090-2099 and 2000-2009. The results show a complex picture of the changes in the circulation, and some of its regional aspects were considered in detail in Popova *et al.* (2016) and Yool *et* *al.* (2015). Of particular importance for this study are the intensification and poleward shift of western boundary currents and a number of more specific regional changes which will be described in the following sections. Circulation Changes are also present in the vertical component and represent a major research topic in its own right that lie beyond the scope of this study.

Metric 1: coastal retention level

Between decades 2000s (2000-2009) and 2090s (2090-99), pronounced changes in coastal retention levels are observed for a large number of coastal regions (Fig. 5a). Regions of largest increase in particles with coastal origin (>15%) are located along the north-eastern Canadian, southern Greenland coast and north-western European coast. In the southern Hemisphere, the Tasmanian and Chilean coast are most affected. In contrast largest decrease of particles with coastal origin (< 20 %) are projected along the north west African coast and the northern coastal parts of the Baffin Bay region. All these changes highlight regions where patterns of connectivity are projected to be modified.

Metric 2: Dominant latitudinal direction

Between decades 2000s and 2090s, pronounced changes in the dominant latitudinal direction of the flow are observed for a large number of coastal regions (Fig. 5b). By the 2090s, these can increase or decrease by up to 20% compared to the 2000s. The largest changes are projected to occur in the southern hemisphere, where there is a predominant increase in poleward flow. By the end of the century, most coastlines will be dominated by poleward displacement of particles (Fig. S4). Large clusters of coastline sites where increases are larger than elsewhere (i.e. >15% more particles moving polewards) form along the major western boundary currents: along the East Australian Current (East Tasmania mostly); along the

Brazil Current and its confluence with the Falklands Current (south east coast of South America); but not along the Agulhas Current, where poleward displacement is already strong. Interestingly, poleward displacement also occurs along eastern boundary currents, notably along the Humboldt and the Benguela currents, due to near-shore surface subtropical waters propagating further south. These changes lead all continental coasts (South America, Africa and Australia) below 15°S to be dominated by poleward displacement.

In the northern hemisphere, the main changes correspond to an intensification of equatorward flow along eastern boundary currents (Western Europe, Northwest Africa and California). Entire stretches of coastlines from France to Mauritania become predominantly equatorward (<10 % of particles moving poleward; Fig. S4). Along the western boundary currents of the Kuroshio and Gulf Stream, only localised changes occur, largely due to shifts in the positions of the locations where these currents leave the coast. Another interesting area is the Azores, where dominant current direction changes from equatorward (more than 80% of particles for all islands) to a more even distribution (40 to 80% of particles).

Metric 3: Changes in dispersal range

Figure 5c shows the difference in poleward range metrics between the 2000s and 2090s. This metric is calculated for the 99th percentile of the longest range particles and thus refers to the extreme component of the flow rather than its average. Globally, patterns appear in the form of localized strong changes. The strongest intensification of poleward pathways occurs in the southern hemisphere in the vicinities of Tasmania, Uruguay, and Chile. In these areas, the intensification of the poleward pathways leads to the expansion of the dispersal range by 7-10 degrees latitude over the standard six month period by the end of the century. In contrast, a weakening is observed for the New Zealand’s North Island. In the northern hemisphere, the most pronounced changes occur in regions of strong weakening. These are located primarily in the Caribbean Sea and along the eastern US coast, areas affected by the North Brazil Current and Gulf Stream, respectively.

Global ocean circulation changes also affect the equatorward range covered by particles reaching coastal regions (Fig. 5d). Similar to changes in poleward range, areas of large changes in equatorward range also appear. In the southern hemisphere, areas of weakening of equatorward pathways form along the North Brazil Current and along the Brazil Current. Equatorward range decreases by 7-10 degrees in these areas. The strongest equatorward intensification (an increase in range of 7-10 degrees) occurs in the northern hemisphere in the subpolar North Atlantic regions around Baffin Island, western Greenland and Iceland, where coasts are exposed to intensifying southward-flowing currents.

Areas facing most pronounced changes

Our analysis identified areas of particularly pronounced circulation changes. In addition to south-east Australia where strong changes are already observed, the regions of strongest circulation changes include Humboldt Current system, Brazil-Falklands Confluence and Baffin Bay/Labrador Sea area (see Fig. S5-S7).

The east Australian region illustrates how complex the effect of ocean circulation changes can be on the connectivity of coastal regions (Fig. 6). The poleward flowing East Australian Current separates south of Sydney into the broad eastward-flowing Tasman front and a residual southern extension of the EAC – mainly consisting of south-propagating eddies (Ridgway, 2007; Suthers *et al.*, 2011). The model shows that the coasts of eastern Australia is connected to the northern tip of the North Island, New Zealand, on timescales shorter than 6 months whereas it does not connect to the southern Tasmanian coast as particles in that area predominantly originate from the west. However, by the end of the century, the projected intensification of the southern branch of the EAC and the weakening of the Tasman front threatens to modify these connectivity patterns. In the model, the intensification of the EAC extension propagates tropical waters as far as the southern Tasmanian coast and consequently connects the region with the East Australian shelf. For 6-month timescales, the flow could potentially transport particles into the region from coastal regions as far as 25° further north. In contrast, the weakening of the Tasman front will reduce the connectivity between the coastal shelves of the New Zealand and East-Australia with connectivity on 6 month-timescale being lost between the two shelves.

Another area of strong projected changes is the Humboldt Current system off the coast of Chile, which supports one of the world largest fisheries (Bakun & Weeks, 2008; Fig. S5). The impact of climate change on the Humboldt ecosystem is already perceptible with an observed expansion of the oxygen minimum zone (Kalvelage *et al.*, 2013). Our results point towards an overall intensification of poleward pathways due to subtropical waters propagating further south at the surface and a modification of the position (southward shift) of the West Wind Drift Current (Robinson & Brink, 1998) – from where the equatorward-flowing Humboldt Current forms. On 6-month timescales, these projected changes increase the potential of tropical species to disperse poleward but also increase the overall proportion of poleward displacement. In contrast, around the Caribbean region, the projected weakening of the North Brazil Current point towards a potential decrease in poleward pathways feeding into the region.

Climate-driven changes projected in the subpolar North Atlantic will also reshuffle present-day dispersal pathways of nearby coastal regions. With the reduction of sea-ice and the intensification of the Arctic circulation (Giles, 2012), the model projects that the equatorward-flowing West Greenland and Baffin Island currents will intensify making it more difficult for coastal species to move against the flow and follow their thermal niche (Fig. S6). These also threaten to completely alter the coastal connectivity patterns of the entire region (Fig. 5a).

Other areas of potential large dispersal pathway changes are regions of coastal separation of western boundary currents (e.g. Kurushio, Gulf Stream) and regions of confluence of major currents (e.g. Brazil-Uruguayan coast). The shift in position of these features exposes these regions to abrupt changes in the origin of incoming water masses with potential strong stresses on the local marine ecosystem. Although localised at the global scale, the sections of coast affected in this way can still stretch hundreds of kilometres (Fig. S7). Note also that these regions are exposed to enhanced warming, where the presence of fronts act as barriers for range boundary extension and where displacement of isotherms is non uniform (Sen Gupta 2016). This picture is therefore a substantial simplification considering that ocean circulation and temperature are not independent.

Discussion

Ocean currents play a critical role in the distribution of marine species by affecting the transport and dispersal of their planktonic propagules. Under the impact of anthropogenic climate warming, ocean circulation has already changed considerably (Wu *et al.*, 2013), and additional change is projected over the 21st century (e.g. Drijfhout *et al.*, 2015; Sen Gupta *et al.*, 2016). Consequently, climate-driven ocean circulation changes will likely modulate the nature of potential pathways (trajectories) taken by coastal marine species and their dispersal agents. In parallel, other climate stressors such as increased temperature or ocean acidification may also impact their survival.

Flow direction matters for marine species as dispersal plays a role in setting (and resetting) range boundaries (Sexton *et al.*, 2009). Dispersal ability has been implicated in facilitating faster range extensions in marine invertebrates (Sunday *et al.*, 2015). Given, to first order, the poleward direction of climate change, it is important to identify whether coastal areas are exposed to currents that are aligned with, or in opposition to, the direction of climate change (Byers & Pringle, 2006; Pringle *et al.*, 2011; Sorte, 2013). Currents aligned with climate change may assist the relocation of species at poleward range edges; however, the same phenomenon may actually hinder retention of larvae at the warming and vulnerable equatorward range edge of the same population (Fig. 7a). For currents prevailing in the direction opposing climate change, the opposite would occur – hindering of dispersal at the poleward range edge where new regions may become thermally appropriate for the species, yet possibly greater larval retention in warming equatorward range edges where populations may be declining in performance (Fig. 7b). The coincidence or otherwise of prevailing patterns of current direction and warming may therefore confer differing risks for warming ecosystems.

Although the body of observational evidence on the importance of potential change in the ocean currents is growing (Verges *et al.*, 2014), modelling studies considering climatically-driven ecological change in the ocean circulation remain relatively rare. A number of regional modelling efforts have addressed the impact of changing currents on the ecosystems around Australia, where the strongest recorded changes are observed (Coleman *et al.*, 2011, 2014;

Cetina-Heredia *et al.*, 2015). However, synoptic, global-scale modelling studies are taking only their first steps in considering ocean circulation as a potential stressor of marine ecosystems (Popova *et al.*, 2016). This is perhaps unsurprising given that a resolution of at least 1/4° is required to reproduce the boundary current features that are critical for understanding the impact of ocean circulation on ecosystems (Hasumi *et al.*, 2014). To put this in context, IPCC AR4 employed models with a typical resolution of 2-3°, and this progressed to around 1° in AR5 (Hasumi *et al.*, 2014), but it is only in AR6 – and then only in a subset of simulations – that 1/4° models will be used. On a related point, horizontal resolution in coupled ocean-atmosphere models supporting IPCC assessments lags behind that of ocean-only models forced by atmospheric fields, which are typically several steps ahead. While these lack some important ocean-atmosphere feedbacks, they provide an acceptable compromise for addressing stressors – such as ocean circulation – that require high resolution (Popova *et al.*, 2016). Against this backdrop, the present study employs such a model forced under IPCC scenario RCP 8.5 to investigate changes in ocean circulation in a systematic way relevant to the potential redistribution of species.

Our analysis focused on the timescale of 6 months and was designed to be most relevant to species with a pelagic larval durations (PLD) of approximately this period. This includes invertebrate groups such as gastropods (e.g. Giant Triton *Cymatium parthenopeum* = 10 months; Shanks *et al.*, 2003), crabs (e.g. Dungeness Crab *Cancer magister* = 3-4 months; Shanks, 2009), spiny lobsters (one year, Matsuda *et al.*, 2006; Rudorff *et al.*, 2009), and fish (e.g. Black Rockfish *Sebastes melanops* = 3-6 months; Shanks, 2009). We demonstrated that at these timescales, dispersal from coastal locations has a basin-scale domain of influence, which might thus be greatly affected by change in large-scale ocean currents. Although the trajectories in our analysis automatically included shorter and longer timescales – from days to 12 months – conclusions regarding periods of one month or less are problematic. The dynamics of inner shelf and coastal zone – which become the dominant domain when considering shorter timescales – remain poorly represented despite the improved resolution relative to existing climate models. Processes associated with, for instance, the shelf break and tidal cycling are missing, and it is likely that they will play a key role in some locales.

Our metrics – following the framework of Sorte (2013) arguing for the importance of the flow patterns when assessing population vulnerability – describe the dispersal range over a 6-month period (also reflective of the speed or intensity of the flow) and directionality (fraction of the flow pathways directed poleward and equatorward). However, we expand the approach here by suggesting that climatically-driven changes in the circulation – even in the absence of other environmental change – can put a pressure on marine ecosystems and need to be taken into account in assessment of ecosystem vulnerability.

In this vein, we consider not only present-day ocean circulation but also its projected change by the last decade of this century. The resulting metrics are rich in regional detail, but general global trends also begin to emerge. For instance, our results show that in the strongest currents, dispersal can reach up to 30° latitude in 6 months, in both poleward and equatorward directions, and thus are much faster than predicted by approaches of location-matching climate velocities (Burrows *et al.*, 2011). We also show that the strongest poleward dispersal is not always associated with the western boundary currents. Although the Gulfstream, Kuroshio, Agulhas, and East Australian Currents show fast poleward displacement, the Brazil Boundary Current with its weaker and more eddy-driven flow does not. Likewise, equatorward counterexamples such as the East Arabian and Caribbean

Currents show equatorward dispersal that is as strong and affects equally large areas as these four boundary current examples.

Even where coastal areas are dominated by strong well-defined currents, upstream dispersal remains possible because of the highly chaotic nature of circulation. In fact, strong unidirectional transport – which we define as > 90% of the Lagrangian pathways going in the same direction (Metric 2) – only occurs in 28% of the global shelf areas studied here. Even in these regions, upstream dispersal of at least 1 or 2 degrees latitude over 6 months timescale is possible. Nonetheless, it can be expected that areas characterised by unidirectional equatorward flow would be most vulnerable to the impact of the global warming. These areas are situated in the vicinity of the equatorward flanks of the subpolar gyres, and are best exemplified in the areas dominated by the Oyashio Current in the Northern North Pacific and the Labrador and East Greenland Currents in the Northern North Atlantic. The latter case, affecting the east coasts of Greenland and west coast of Canada, provides the most notable example of unidirectional and uninterrupted equatorward flow, one which impacts thousands kilometres of coastline. Furthermore, circulation changes are predicted to intensify this pattern. We suggest that in these areas of the Northern North Atlantic, the first observational evidence of temperature-driven and circulation-mediated extinctions of marine species may emerge much earlier than in other areas. These conclusions would not have been reached by simply analysing Eulerian motions alone.

While the preceding discussion focused on the present state of the ocean, both flow directionality and flow-driven dispersal range (equator- and pole-ward) are projected to experience significant change during the 21st century. This is sometimes aligned with the poleward pattern of ocean warming (i.e. dispersal carrying particles away from warming waters is enhanced), and sometimes is in opposition to it (i.e. dispersal carrying particles towards warming water is enhanced). The former may assist species in "keeping up with" their thermal habitat, while the latter is more likely to impede compensatory dispersal and range shifts for species living in these areas. We show that the most pronounced example of climatically-driven circulation changes is associated with the projected weakening of the eastward and strengthening southward components of the East Australian Current, leading to the loss of connectivity between east Australian coast and New Zealand on a time scale of six months considered in this study. This specific change in circulation may reduce connectivity of rock lobster populations and the sustainability of their fisheries (Bradford *et al.*, 2015).

More generally, even in cases where the bulk ocean circulation changes in a manner that hinders species dispersal, it may still be possible for species to track their shifting thermal habitat. As noted above, and in almost all cases here, some simulated particles were found to travel "against the flow", due to persistent inshore counter-currents that may only be partially represented in the ocean model, or episodic reversals of the major coastal current. These inshore currents are difficult to simulate accurately since they can be narrower than the model grid resolution (even at ¼°), and, like other currents, are also often episodic (Hobday & Lough, 2011, Stock *et al.*, 2011). Persistence in advective habitats requires adaptations simply to preserve existing range boundaries, such as releasing propagules during seasons of lowest flow speeds or highest flow variability (Byers & Pringle, 2006).

There are, inevitably, caveats to this study. The physical model used is primarily an open ocean model, and omits processes such as tides that are important in shallow, inshore waters. Higher resolution regional models that include these processes represent one solution to this, though they lose the large-scale interconnectedness permitted by a global GCM.

Additionally, due to the cost of high resolution simulation, a contrasting control run that does not experience climate change (cf. a longer spin-up) has been precluded here. More generally, our study makes use of the simulated circulation from a single model only, and our analysis is not able to include estimates of model uncertainty derived from multiple simulations. A common factor in these limitations is computing resource, which affect the duration and resolution of possible simulations (the latter additionally affects the processes that can be represented). Consequently, it may be expected that improvements in the future availability of computing resources will decrease the significance of the limitations experienced here, and permit more complete analyses of the important of changing circulation.

The numerical approach adopted in this study was designed to maximise applicability of the results to as many species as possible, while working in a systematic way across the global ocean's shelf regions. By necessity, this approach simplifies or overlooks a number of features of importance for population dynamics. First of all, marine organisms are not entirely passive and are characterised by a range of behaviour, such as diel vertical migration, via swimming or changes in buoyancy. Larvae located at different depths will be subject to different currents (Werner *et al.*, 2007), and thus connectivity and retention can be modulated by the behaviour of organisms (Gerber *et al.*, 2014). Additionally, in terms of species connectivity and species redistribution under a changing climate, many species are highly mobile in adult phases where the relative energy expenditure to move against prevailing currents would be lower than for smaller stages. So while we have focused on larval dispersal as a means of "tracking" a thermal habitat, many species may instead do so when adults. More generally, our analysis has dealt with larval dispersal without directly considering the thermal habitats relevant to species. For instance, it is interesting to consider whether shorter dispersal trajectories in the future span a smaller or larger range of temperatures, or whether a change in circulation coincides with a corresponding change in temperature or even oxygen. These simplifications have been made to permit a first-order investigation of how changing ocean circulation could affect planktonic mobility into the future, and – in part by omission – to suggest where future research may be targeted.

In summary, a growing number of recent modelling and conceptual studies are dedicated to the assessment of the impact of climate change on marine ecosystems (e.g. Gruber, 2011; Doney *et al.*, 2012; Bopp *et al.*, 2013; Mora *et al.*, 2013; Popova *et al.*, 2016, Marzloff *et al.*, 2016). The four most widely recognized stressors (or drivers of change) impacting marine life are rising ocean temperatures, ocean acidification, de-oxygenation and changes in primary production. We have shown that changes to ocean circulation pathways can also strongly impact marine ecosystems through the redistribution of species, and argue that observational evidence of these changes is beginning to emerge. Consequently, we suggest that climatically-induced changes in ocean circulation should be considered as an additional stressor of marine ecosystems in a similar way as ocean warming or acidification. As a first step towards this goal, we have presented results based on three metrics that can assess these changes in a systematic way across marine species. As spatial resolution of climate models increases and realism of the ocean circulation in these models improves, model intercomparison studies and uncertainty analyses will be needed to assess robustness of the spatial patterns presented here. Through this, we will better be able to assess and reduce uncertainty in future modelling projections of the impact of ocean circulation on marine species and ecosystems.

Acknowledgments

We are grateful for funding provided under the Belmont Forum by national and regional science agencies, including CSIRO and the University of Tasmania Institute for Marine and Antarctic Studies (Australia) and NERC (UK), within the framework of the international GULLS project (NSF code G8MUREFU3FP-2201-081). GTP was supported by an ARC Future Fellowship. The modelling work was supported by NERC National Capability funding (NEW322900), the Strategic Research Impact project (SIRENA; NE/M00693X/1) and the Regional Ocean Acidification Modelling project (ROAM; NE/H017372/1). This work used the ARCHER UK National Supercomputing Service (*http://www.archer.ac.uk*) for the high resolution component of the modelling. Lagrangian analysis was carried out using computational tool Ariane developed by B. Blanke and N. Grima.

References:

Bakun A, Weeks SJ (2008) The marine ecosystem off Peru: What are the secrets of its fishery productivity and what might its future hold? Progress In Oceanography, **79**, 290-299.

Banks SC, Ling SD, Johnson CR, Piggott MP, Williamson JE, Beheregaray LB (2010) Genetic structure of a recent climate change-driven range extension. Molecular Ecology, **19**, 2011-2024.

Bates AE, Pecl GT, Frusher S *et al.* (2014) Defining and observing stages of climate-mediated range shifts in marine systems. Global Environmental Change, **26**, 27-38.

Blanke B, Raynaud S (1997) Kinematics of the Pacific Equatorial Undercurrent: An Eulerian and Lagrangian Approach from GCM Results. Journal of Physical Oceanography, **27**, 1038-1053.

Bopp L, Resplandy L, Orr JC *et al.* (2013) Multiple stressors of ocean ecosystems in the 21st century: projections with CMIP5 models. Biogeosciences, **10**, 6225-6245.

Botsford LW, Moloney CL, Hastings A, Largier JL, Powell TM, Higgins K, Quinn JF (1994) The influence of spatially and temporally varying oceanographic conditions on meroplanktonic metapopulations. Deep Sea Research Part II: Topical Studies in Oceanography, **41**, 107-145.

Bradford RW, Griffin D, Bruce BD (2015) Estimating the duration of the pelagic phyllosoma phase of the southern rock lobster, Jasus edwardsii (Hutton). Marine and Freshwater Research, **66**, 213-219.

Brink KH, Robinson AR (1998) *The Global Coastal Ocean: Processes and Methods,* New York, John Wiley & Sons,.

Burrows MT, Schoeman DS, Buckley LB *et al.* (2011) The Pace of Shifting Climate in Marine and Terrestrial Ecosystems. Science, **334**, 652-655.

Byers JE, Pringle JM (2006) Going against the flow: retention, range limits and invasions in advective environments. Marine Ecology Progress Series, **313**, 27-41.

Cetina-Heredia P, Roughan M, Van Sebille E, Feng M, Coleman MA (2015) Strengthened currents override the effect of warming on lobster larval dispersal and survival. Global Change Biology*,* **21**, 4377-4386.

Clarke AJ (2013) Poleward Flow In The California Current System. In: *Poleward Flows Along Eastern Ocean Boundaries.* pp Page., Springer-Verlag.

Coleman MA, Feng M, Roughan M, Cetina-Heredia P, Connell SD (2013) Temperate shelf water dispersal by Australian boundary currents: Implications for population connectivity. Limnology and Oceanography: Fluids and Environments*,* **3**, 295-309.

Coleman MA, Roughan M, Macdonald HS, Connell SD, Gillanders BM, Kelaher BP, Steinberg PD (2011) Variation in the strength of continental boundary currents determines continent-wide connectivity in kelp. Journal of Ecology*,* **99**, 1026-1032.

Collins WJ, Bellouin N, Doutriaux-Boucher M *et al.* (2011) Development and evaluation of an Earth-System model-HadGEM2. Geoscientific Model Development*,* **4**, 1051-1075.

Cowen RK, Gawarkiewic G, Pineda J, Thorrold SR, Werner FE (2007) Population Connectivity in Marine Systems An Overview. Oceanography*,* **20**, 14-21.

Doblin MA, Van Sebille E (2016) Drift in ocean currents impacts intergenerational microbial exposure to temperature. Proceedings of the National Academy of Sciences*,* **113**, 5700-5705.

Doney SC, Ruckelshaus M, Duffy JE *et al.* (2012) Climate Change Impacts on Marine Ecosystems. Annual Review of Marine Science*,* **4**, 11-37.

Döös K (1995) Interocean exchange of water masses. Journal of Geophysical Research: Oceans*,* **100**, 13499-13514.

Drijfhout S, Bathiany S, Beaulieu C *et al.* (2015) Catalogue of abrupt shifts in Intergovernmental Panel on Climate Change climate models. Proceedings of the National Academy of Sciences*,* **112**, E5777-E5786.

Elrod VA, Berelson WM, Coale KH, Johnson KS (2004) The flux of iron from continental shelf sediments: A missing source for global budgets. Geophysical Research Letters*,* **31**, n/a-n/a.

Gaspar P, Grégoris Y, Lefevre J-M (1990) A simple eddy kinetic energy model for simulations of the oceanic vertical mixing: Tests at station Papa and long-term upper ocean study site. Journal of Geophysical Research: Oceans*,* **95**, 16179-16193.

Gerber LR, Mancha-Cisneros MDM, O'connor MI, Selig ER (2014) Climate change impacts on connectivity in the ocean: Implications for conservation. Ecosphere*,* **5**, 1-18.

Giles KA, Laxon SW, Ridout AL, Wingham DJ, Bacon S (2012) Western Arctic Ocean freshwater storage increased by wind-driven spin-up of the Beaufort Gyre. Nature Geosci*,* **5**, 194-197.

Goldwyn EE, Hastings A (2011) The roles of the Moran effect and dispersal in synchronizing oscillating populations. Journal of Theoretical Biology*,* **289**, 237-246.

Gruber N, Hauri C, Lachkar Z, Loher D, Frölicher TL, Plattner G-K (2012) Rapid Progression of Ocean Acidification in the California Current System. Science*,* **337**, 220-223.

Hassumi H (2014) A review on ocean resolution dependence of climate biases in AOGCMs. CLIVAR Exchanges, 7–9.

Hill KL, Rintoul SR, Coleman R, Ridgway KR (2008) Wind forced low frequency variability of the East Australia Current. Geophysical Research Letters*,* **35**, n/a-n/a.

Hobday AJ, Lough JM (2011) Projected climate change in Australian marine and freshwater environments. Marine and Freshwater Research*,* **62**, 1000-1014.

Hobday AJ, Pecl GT (2014) Identification of global marine hotspots: sentinels for change and vanguards for adaptation action. Reviews in Fish Biology and Fisheries*,* **24**, 415-425.

Hoegh-Guldberg O, Bruno JF (2010) The Impact of Climate Change on the World's Marine Ecosystems. Science*,* **328**, 1523-1528.

IPCC (2013) Summary for Policymakers. In: *Climate Change 2013: The Physical Science Basis. Contribution of Working Group I to the Fifth Assessment Report of the Intergovernmental Panel on Climate Change.* (eds Stocker TF, Qin D, Plattner G-K, Tignor M, Allen SK, Boschung

J, Nauels A, Xia Y, Bex V, Midgley PM) pp Page. Cambridge, United Kingdom and New York, NY, USA, Cambridge University Press.

Johnson CR, Banks SC, Barrett NS *et al.* (2011) Climate change cascades: Shifts in oceanography, species' ranges and subtidal marine community dynamics in eastern Tasmania. Journal of Experimental Marine Biology and Ecology, **400**, 17-32.

Jonsson BF, Watson JR (2016) The timescales of global surface-ocean connectivity. Nat Commun, **7**.

Jutzeler M, Marsh R, Carey RJ, White JDL, Talling PJ, Karlstrom L (2014) On the fate of pumice rafts formed during the 2012 Havre submarine eruption. Nature Communications, **5**, 3660.

Kalvelage T, Lavik G, Lam P *et al.* (2013) Nitrogen cycling driven by organic matter export in the South Pacific oxygen minimum zone. Nature Geosci, **6**, 228-234.

Kendall MS, Poti M, Karnauskas KB (2016) Climate change and larval transport in the ocean: fractional effects from physical and physiological factors. Global Change Biology, **22**, 1532-1547.

Kinlan BP, Gaines SD (2003) Propagule Dispersal in Marine and Terrestrial Environments: A Community Perspective. Ecology, **84**, 2007-2020.

Lett C, Ayata S-D, Huret M, Irisson J-O (2010) Biophysical modelling to investigate the effects of climate change on marine population dispersal and connectivity. Progress In Oceanography, **87**, 106-113.

Ling SD, Johnson CR, Ridgway K, Hobday AJ, Haddon M (2009) Climate-driven range extension of a sea urchin: inferring future trends by analysis of recent population dynamics. Global Change Biology, **15**, 719-731.

Lumpkin R, Maximenko N, Pazos M (2012) Evaluating Where and Why Drifters Die. Journal of Atmospheric and Oceanic Technology, **29**, 300-308.

Madec G (2008) NEMO reference manual, ocean dynamic component: NEMO-OPA. Note du Pôle de modélisation No 27,. pp Page, Institut Pierre-Simon Laplace (IPSL), France.

Main CE, Ruhl HA, Jones DOB, Yool A, Thornton B, Mayor DJ (2015) Hydrocarbon contamination affects deep-sea benthic oxygen uptake and microbial community composition. Deep Sea Research Part I: Oceanographic Research Papers, **100**, 79-87.

Marshall Dustin j, Morgan Steven g (2011) Ecological and Evolutionary Consequences of Linked Life-History Stages in the Sea. Current Biology, **21**, R718-R725.

Marzloff MP, Melbourne-Thomas J, Hamon KG, Hoshino E, Jennings S, Van Putten IE, Pecl GT (2016) Modelling marine community responses to climate-driven species redistribution to guide monitoring and adaptive ecosystem-based management. Global Change Biology, n/a-n/a.

Marzocchi A, Hirschi JJM, Holliday NP, Cunningham SA, Blaker AT, Coward AC (2015) The North Atlantic subpolar circulation in an eddy-resolving global ocean model. Journal of Marine Systems, **142**, 126-143.

Matear RJ, Chamberlain MA, Sun C, Feng M (2013) Climate change projection of the Tasman Sea from an Eddy-resolving Ocean Model. Journal of Geophysical Research: Oceans, **118**, 2961-2976.

Mora C, Wei C-L, Rollo A *et al.* (2013) Biotic and Human Vulnerability to Projected Changes in Ocean Biogeochemistry over the 21st Century. PLoS Biol, **11**, e1001682.

Munday PL, Donelson JM, Dixson DL, Endo GGK (2009) Effects of ocean acidification on the early life history of a tropical marine fish. Proceedings of the Royal Society of London B: Biological Sciences, **276**, 3275-3283.

Okey TA, Alidina HM, Lo V, Jessen S (2014) Effects of climate change on Canada's Pacific marine ecosystems: a summary of scientific knowledge. Reviews in Fish Biology and Fisheries, **24**, 519-559.

Pechenik JA (1999) On the advantages and disadvantages of larval stages in benthic marine invertebrate life cycles. Marine Ecology Progress Series, **177**, 269-297.

Pecl GT, Hobday AJ, Frusher S, Sauer WHH, Bates AE (2014) Ocean warming hotspots provide early warning laboratories for climate change impacts. Reviews in Fish Biology and Fisheries, **24**, 409-413.

Poloczanska ES, Brown CJ, Sydeman WJ *et al.* (2013) Global imprint of climate change on marine life. Nature Clim. Change, **3**, 919-925.

Popova E, Yool A, Byfield V *et al.* (2016) From global to regional and back again: common climate stressors of marine ecosystems relevant for adaptation across five ocean warming hotspots. Global Change Biology, n/a-n/a.

Popova EE, Yool A, Aksenov Y, Coward AC (2013) Role of advection in Arctic Ocean lower trophic dynamics: A modeling perspective. Journal of Geophysical Research: Oceans, **118**, 1571-1586.

Pringle JM, Blakeslee AMH, Byers JE, Roman J (2011) Asymmetric dispersal allows an upstream region to control population structure throughout a species' range. Proceedings of the National Academy of Sciences, **108**, 15288-15293.

Ridgway KR (2007) Long-term trend and decadal variability of the southward penetration of the East Australian Current. Geophysical Research Letters, **34**, n/a-n/a.

Robinson J, Popova EE, Srokosz M, Yool A (2016) A tale of three islands: Downstream natural iron fertilization in the Southern Ocean. Journal of Geophysical Research: Oceans, n/a-n/a.

Robinson J, Popova EE, Yool A, Srokosz M, Lampitt RS, Blundell JR (2014) How deep is deep enough? Ocean iron fertilization and carbon sequestration in the Southern Ocean. Geophysical Research Letters, **41**, 2489-2495.

Rodrigues RR, Rothstein LM, Wimbush M (2007) Seasonal Variability of the South Equatorial Current Bifurcation in the Atlantic Ocean: A Numerical Study. Journal of Physical Oceanography, **37**, 16-30.

Rogelj J, Meinshausen M, Knutti R (2012) Global warming under old and new scenarios using IPCC climate sensitivity range estimates. Nature Clim. Change, **2**, 248-253.

Rudorff CaG, Lorenzzetti JA, Gherardi DFM, Lins-Oliveira JE (2009) Modeling spiny lobster larval dispersion in the Tropical Atlantic. Fisheries Research, **96**, 206-215.

Saunders GW (2014) Long distance kelp rafting impacts seaweed biogeography in the Northeast Pacific: the kelp conveyor hypothesis. Journal of Phycology, **50**, 968-974.

Sen Gupta A, Mcgregor S, Van Sebille E, Ganachaud A, Brown JN, Santoso A (2016) Future changes to the Indonesian Throughflow and Pacific circulation: The differing role of wind and deep circulation changes. Geophysical Research Letters, **43**, 1669-1678.

Sexton JP, Mcintyre PJ, Angert AL, Rice KJ (2009) Evolution and Ecology of Species Range Limits. Annual Review of Ecology, Evolution, and Systematics, **40**, 415-436.

Shanks AL (2009) Pelagic Larval Duration and Dispersal Distance Revisited. The Biological Bulletin, **216**, 373-385.

Shanks AL, Grantham BA, Carr MH (2003) Propagule Dispersal Distance and the Size and Spacing of Marine Reserves. Ecological Applications, **13**, S159-S169.

Siegel DA, Kinlan BP, Gaylord B, Gaines SD (2003) Lagrangian descriptions of marine larval dispersion. Marine Ecology Progress Series, **260**, 83-96.

Sloyan BM, O'kane TJ (2015) Drivers of decadal variability in the Tasman Sea. Journal of Geophysical Research: Oceans, **120**, 3193-3210.

Sorte CJB (2013) Predicting persistence in a changing climate: flow direction and limitations to redistribution. Oikos, **122**, 161-170.

Soutelino RG, Da Silveira ICA, Gangopadhyay A, Miranda JA (2011) Is the Brazil Current eddy-dominated to the north of 20°S? Geophysical Research Letters, **38**, n/a-n/a.

Srokosz MA, Robinson J, Mcgrain H, Popova EE, Yool A (2015) Could the Madagascar bloom be fertilized by Madagascan iron? Journal of Geophysical Research: Oceans, **120**, 5790-5803.

Stock CA, Alexander MA, Bond NA *et al.* (2011) On the use of IPCC-class models to assess the impact of climate on Living Marine Resources. Progress In Oceanography, **88**, 1-27.

Sun C, Feng M, Matear RJ, Chamberlain MA, Craig P, Ridgway KR, Schiller A (2012) Marine Downscaling of a Future Climate Scenario for Australian Boundary Currents. Journal of Climate*,* **25**, 2947-2962.

Sunday JM, Pecl GT, Frusher S *et al.* (2015) Species traits and climate velocity explain geographic range shifts in an ocean-warming hotspot. Ecology Letters*,* **18**, 944-953.

Suthers IM, Young JW, Baird ME *et al.* (2011) The strengthening East Australian Current, its eddies and biological effects — an introduction and overview. Deep Sea Research Part II: Topical Studies in Oceanography*,* **58**, 538-546.

Thompson PA, Baird ME, Ingleton T, Doblin MA (2009) Long-term changes in temperate Australian coastal waters: implications for phytoplankton. Marine Ecology Progress Series*,* **394**, 1-19.

Timmermann R, Goosse H, Madec G, Fichefet T, Ethe C, Duliere V (2005) On the representation of high latitude processes in the ORCA-LIM global coupled sea ice-ocean model. Ocean Modelling*,* **8**, 175-201.

van Gennip SJ, Popova EE, Yool A, Pecl G, Hobday A, Sorte CJB (2017) Data from: Going with the flow: The role of ocean circulation in global marine ecosystems under a changing climate. Global Change Biology. http://dx.doi.org/10.5061/dryad.233hb

Vergés A, Steinberg PD, Hay ME *et al.* (2014) The tropicalization of temperate marine ecosystems: climate-mediated changes in herbivory and community phase shifts. Proceedings of the Royal Society of London B: Biological Sciences*,* **281**.

Walsh JJ (1991) Importance of continental margins in the marine biogeochemical cycling of carbon and nitrogen. Nature*,* **350**, 53-55.

Wang FC, Wu HA, Geim AK (2015) Wang et al. reply. Nature*,* **528**, E3-E3.

Wassmann P, Duarte CM, Agustí S, Sejr MK (2011) Footprints of climate change in the Arctic marine ecosystem. Global Change Biology*,* **17**, 1235-1249.

Werner FE, Cowen RK, Paris CB (2007) Coupled Biological and Physical Models Present Capabilities and Necessary Developments for Future Studies of Population Connectivity. Oceanography*,* **20**, 54-69.

Wu L, Cai W, Zhang L *et al.* (2012) Enhanced warming over the global subtropical western boundary currents. Nature Clim. Change*,* **2**, 161-166.

Yool A, Popova EE, Coward AC (2015) Future change in ocean productivity: Is the Arctic the new Atlantic? Journal of Geophysical Research-Oceans*,* **120**, 7771-7790.

Yool A, Popova EE, Coward AC, Bernie D, Anderson TR (2013) Climate change and ocean acidification impacts on lower trophic levels and the export of organic carbon to the deep ocean. Biogeosciences*,* **10**, 5831-5854.

Figure captions

Fig. 1: Global distribution of decadal-averaged surface current speed (m s^{-1}) for the period 2000-09 from (a) AVISO satellite estimates and (b) NEMO model output. Panel (c) shows the relative change (m s^{-1}) in decadal-average modelled current speed between the 2000s and the 2090s.

Fig. 2: (a) Illustration of the spatial scales associated with particles being advected for a 6-month period. Trajectories are from a subsample of 50 km coastal sections of the global release, and show particles approximately every 1500 km along the global coast and backtracked for 6 months. Particle release sites and associated trajectories have matching colours. Release sites were placed in a ribbon-

like manner 70 km away from the coastline (red line) at 1 km interval. For the analysis, sites were grouped into 50 km sections (illustrated in color in the zoom around Tasmania). Particles were released quarterly and advected for as long as 12 months for the decades 2000-09, 2050-59 and 2090-99. A regional example from a section of the Tasmanian coast is shown for each decade: (b) 2000s, (c) 2050s, (d) 2090s. Here, the colours denote the time elapsed from the release. Since particles are advected backward in time, the purple colour (month 12) indicates their origin while the red colour (month 1) indicates the area where the trajectories are converging to.

Fig. 3: Illustration of the metrics developed using an ensemble of trajectories from particles released within a section off the coast of Chile (green dot) and advected backward in time for 6 months. For each trajectory (see bottom right subpanel), points closest to the pole (blue dots) and to the equator (red dots) and within coastal waters are identified to generate two data sets: most poleward and most equatorward points. The most poleward and equatorward 1% of points in each data set (red and blue diamonds, respectively) are then used to calculate the maximum poleward (7.0°) and equatorward (5.6°) displacement completed by particles to reach the destination site. Note that with backtracked trajectories, the most equatorward particle position indicates the longest poleward journey to reach the coastal site. The dominant latitudinal direction (bottom left subpanel in red), here 29%, corresponds to the proportion of particles travelling poleward. Coastal waters are within 85 km from the shoreline (orange ribbon).

Fig. 4: Global coastal distribution of metrics for the period 2000-09 using 6-month backtracked trajectories. Panel (a): Proportion of particles originating from coastal waters (6 month before reaching given site). Panel (b): dominant latitudinal direction of the flow (percentage of particles moving poleward). Values larger (smaller) than 50% correspond to poleward (equatorward) dominated flow and represented in warm (cold) colours. Panel (c): maximum displacement in the poleward direction (in degrees latitude) of particles arriving to a coastal site after 6 months of being released. In the north (south) hemisphere, this corresponds to the displacement (in degrees latitude) in the equator to north-pole (south-pole) direction. Panel (d): same as Panel (c), but instead focusing on particles that have travelled in the equatorward direction. Trajectories (grey lines) in the background

represent the major ocean circulation features of the model, with longer lines corresponding to the faster currents. Note that uncoloured coastal stretches were not included in this study.

Fig. 5: Projected changes between decades 2000s and 2090s for the metrics developed. Panel (a): Proportion of particles originating from coastal waters (6 month before reaching given site). Panel (b): dominant latitudinal direction of the flow, with warm (cold) colours corresponding to an increase (decrease) in poleward flow. Panel (c): maximum displacement in the poleward direction, with warm (cold) colours corresponding to an intensification (weakening) in poleward displacement potential (in degrees latitude). Panel (d): as Panel (c) but for the equatorward direction.

Fig. 6: Example of the effect of ocean circulation changes on two coastal sites along the East Australian Current (EAC) between (a) decades 2000-09 and (c) 2090-99. For the Tasmanian release, the projected intensification of the southern branch of the EAC leads to both an increase of the maximum poleward displacement (+14°; from +7° to +21°) and to changes in the connectivity with the Australian shelf (from the south to the northeast coast). In contrast, the projected weakening of the Tasman front decreases the maximum poleward displacement (-9°; from +10° to +1°) with a disruption in connectivity between the Australian and New Zealand shelves on the 6-month timescale shown. The 85 km from the shore ribbon (orange) separate coastal and open waters. For illustration, the present model NEMO current speed (b) and the deviation of decadal average speeds for the period 2090-2099 from 2000-09 (d) are also shown.

Fig. 7: Potential effect of current direction on the distribution of propagules (red dots and line) of species chasing their thermal niche in a warming climate. Panel (a): the flow is aligned with climate change and assists species dispersal at poleward range edges. Panel (b) the flow opposes climate change and hinders dispersal at the poleward edges with greater propagules at the warming equatorward edges. The filled blue (dashed green) area depicts the present (future) region thermally appropriate for the species. This diagram was adapted from Sorte (2013).

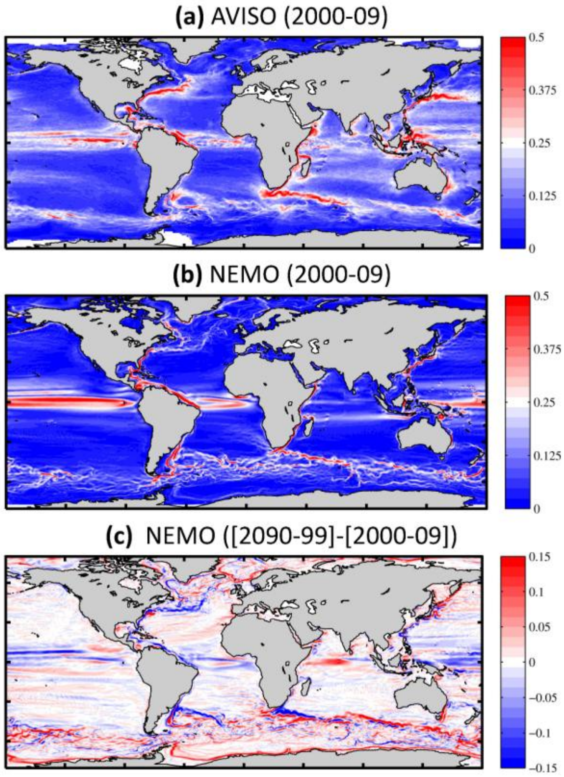
(a) AVISO (2000-09)
0.5
0.375
0.25
0.125
0
(b) NEMO (2000-09)
0.5
0.375
0.25
0.125
0
(c) NEMO ([2090-99]-[2000-09])
0.15
0.1
0.05
0
−0.05
−0.1
−0.15

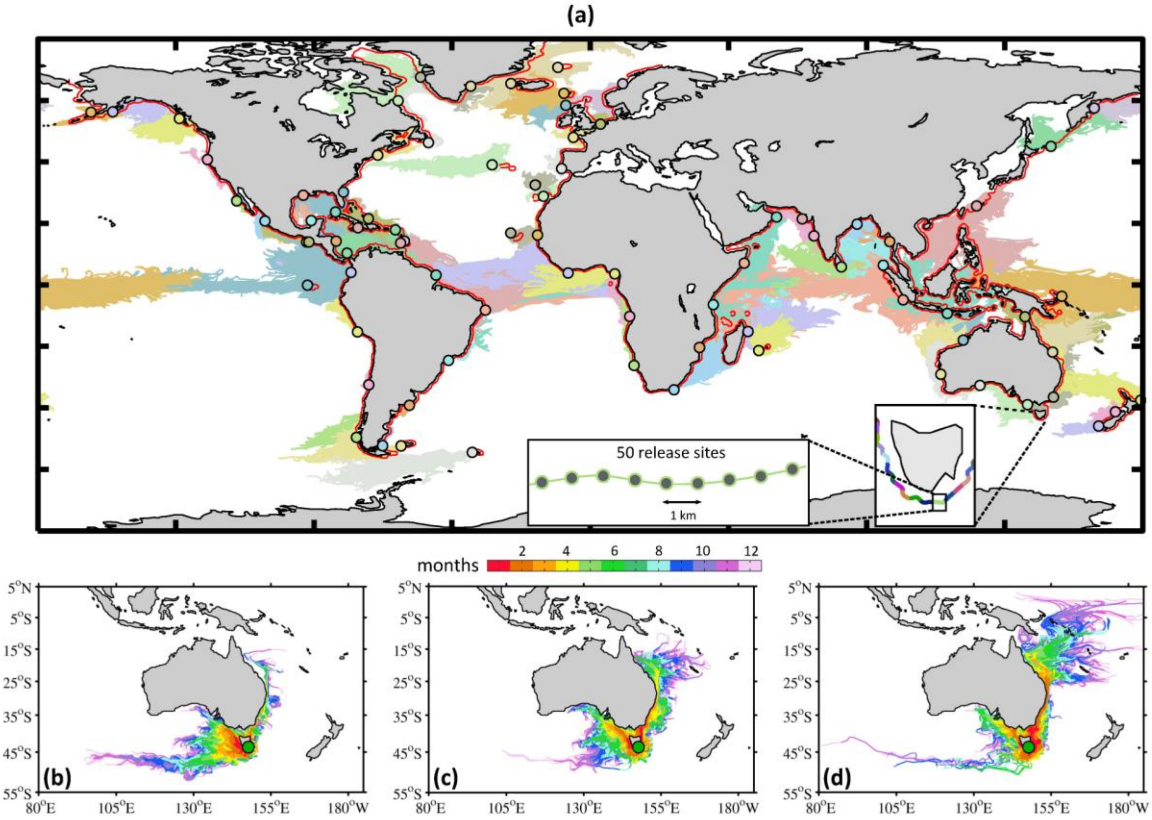
(a)
50 release sites
1 km
months
2
4
6
8
10
12
5°N
5°S
15°S
25°S
35°S
45°S
55°S
80°E
105°E
130°E
155°E
180°W
(b)
(c)
(d)

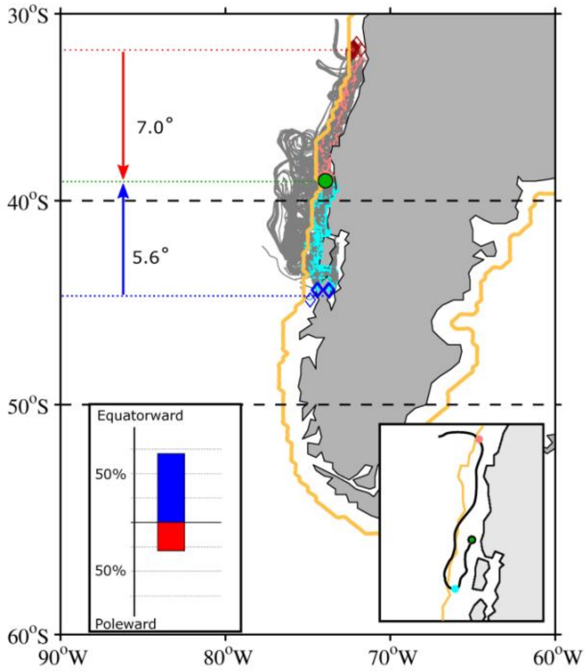
30°S
40°S
50°S
60°S
90°W
80°W
70°W
60°W
7.0°
5.6°
Equatorward
50%
50%
Poleward

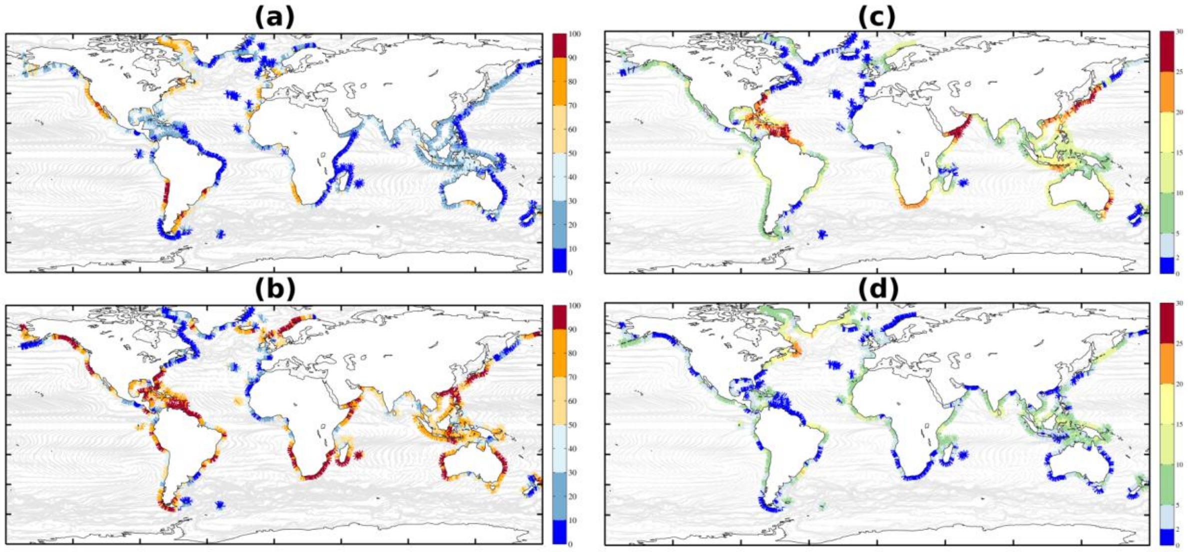
(a)
(b)
(c)
(d)
0
10
20
30
40
50
60
70
80
90
100
0
2
5
10
15
20
25
30

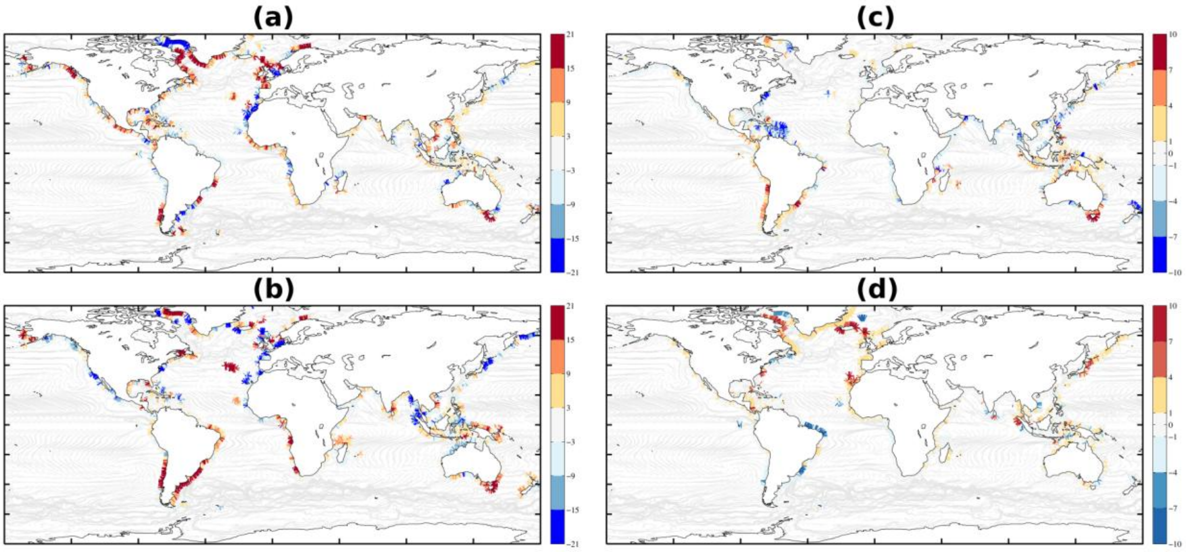
(a)
(c)
(b)
(d)
21
15
9
3
−3
−9
−15
−21
10
7
4
1
0
−1
−4
−7
−10

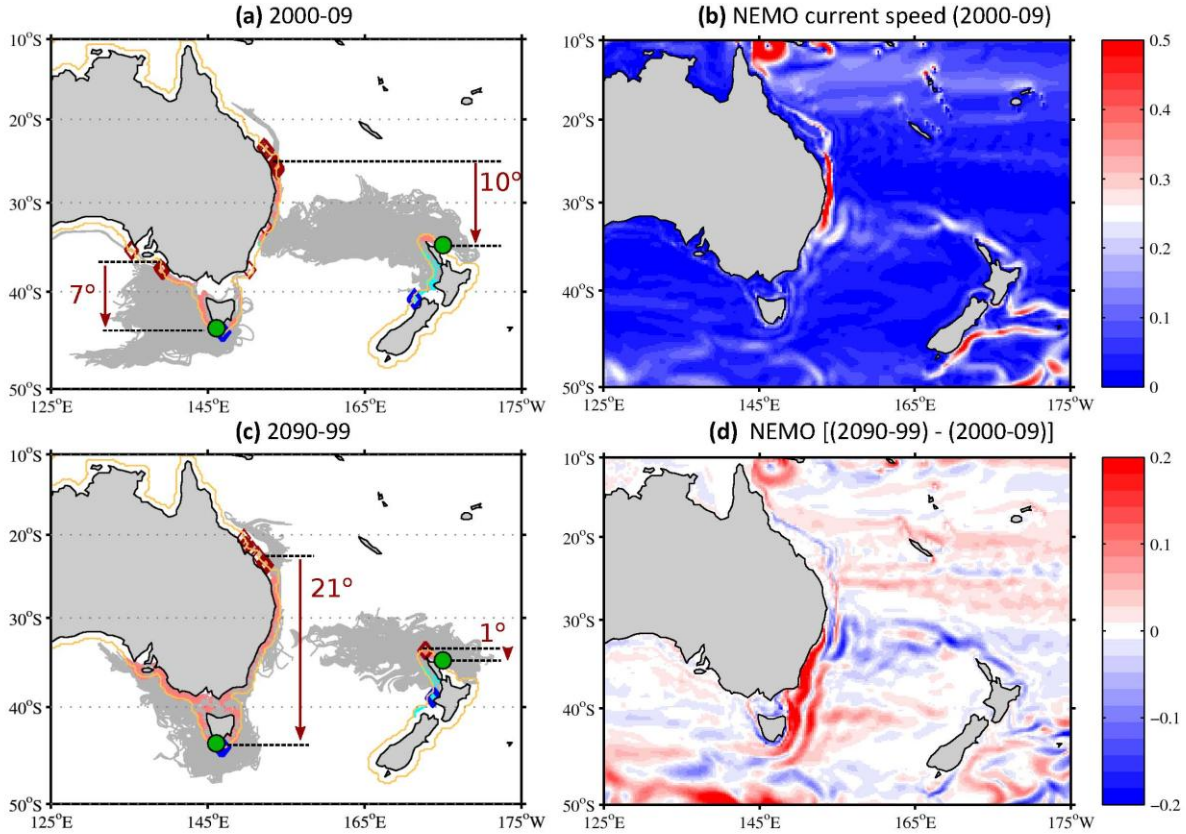
(a) 2000-09
(b) NEMO current speed (2000-09)
(c) 2090-99
(d) NEMO [(2090-99) - (2000-09)]
10°
7°
21°
1°
10°S
20°S
30°S
40°S
50°S
125°E
145°E
165°E
175°W
0.5
0.4
0.3
0.2
0.1
0
0.2
0.1
0
−0.1
−0.2

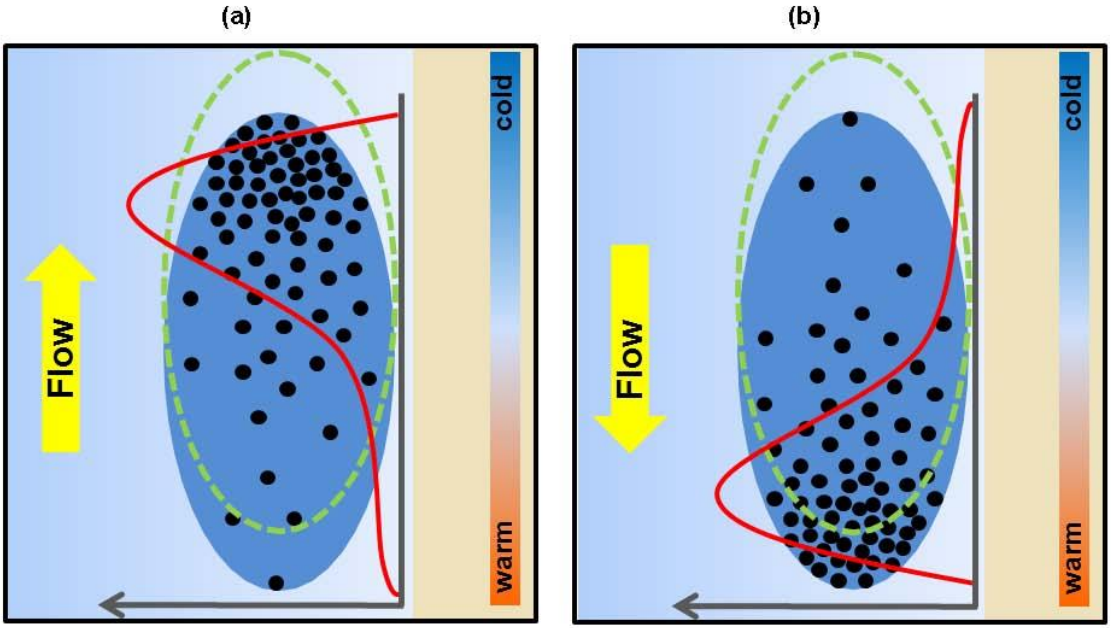
(a)
Flow
cold
warm
(b)
Flow
cold
warm